American Astronautical Society

**AIAA**
American Institute of
Aeronautics and Astronautics
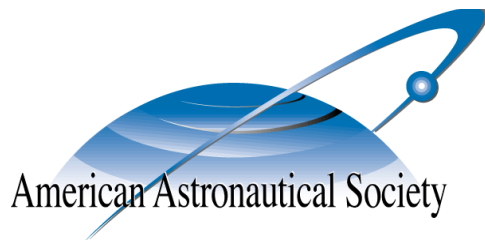
# COULOMB SPACECRAFT VOLTAGE STUDY DUE TO DIFFERENTIAL ORBITAL PERTURBATION

C.C. Romanelli , A. Natarajan , H. Schaub , G.G. Parker and L.B. King

# 2006 AAS/AIAA Space Flight Mechanics Meeting

Tampa, Florida        Jan. 22–26, 2006

# COULOMB SPACECRAFT VOLTAGE STUDY DUE TO DIFFERENTIAL ORBITAL PERTURBATION

## C.C. Romanelli[*], A. Natarajan[†], H. Schaub[‡], G.G. Parker[§]and L.B. King[¶]

The effects of differential atmospheric drag, $J_2$ perturbations, and solar radiation drag on the relative motion of a small formation of satellites is examined. Nonlinear simulations in the inertial frame are used to determine the worst case differential orbital perturbations relative to the drifting formation center of mass location. Varying the nominal separation distances between 10–1000 meters and the altitude from LEO to GEO, a profile of the dominant perturbation zones is developed. A study is also provided to compute Lorentz force acceleration of a charged spacecraft in Earth's magnetic field. Two formation types are considered when computing nominal spacecraft voltages to compensate for these perturbations. First, using a traditional formation flying approach all spacecraft are allowed to interact with each other. Minimal charge products are computed to determine the worst expected voltage levels. Second, a gluon-deputy craft combination is studied. Here a much larger gluon craft is specifically designed to be able to handle much larger voltages. This allows the deputies to have lower voltage levels to achieve the same force. A study is performed to illustrate how the required gluon charge levels will vary with different gluon radii, as well as different Debye lengths.

## INTRODUCTION

The perturbations that many aerospace engineers deal with in normal orbit operations can have a large effect on the relative motion of two closely orbiting satellites. In Reference 1 a study is done on the long term effects of perturbations on the DRAIM satellite constellation. The results clearly indicate that after 10 years, orbit perturbations have a significant effect on the relative motion of this constellation. However, the goal of this study is to examine the effects of perturbations on formations on the order of 10 to 1000 meters. The applications range from wide field-of-view interferometry, to forming virtual structures, to engaging in close proximity flying operations, as well as rendezvous and docking maneuvers. The traditional control solution would be to use thrusters, which not only expend a large amount of fuel, but also the exhaust plume produced can damage sensors or delicate equipment on nearby spacecraft. In Reference 2, the concept of using Coulomb forces to control satellite formations is investigated. This work determined that spacecraft generating a relative potential of a few kilo-volts would be sufficient to produce inter-spacecraft forces on the order of micro- to milli-newtons. This amount of force is enough to continuously control the spacecraft with a large impulse.

However, there are challenges to using spacecraft charging in this manner. Earth's ambient plasma environment can effect the performance of these Coulomb forces. King and Parker[3] showed that at higher Earth orbits the Debye length is on the order of 100's of meters, which allows for a reasonable environment to use Coulomb forces. However, at low Earth orbits (LEO) the Debye length becomes much smaller and can greatly effect the charging characteristics of the spacecraft. The Debye length is a measure of the distance over which charged particles produce Coulomb forces. The shorter the

---

[*]Masters Student, Aerospace and Ocean Engineering Dep., Virginia Tech, Blacksburg, VA 24060
[†]Ph.D Student, Aerospace and Ocean Engineering Dep., Virginia Tech, Blacksburg, VA 24060
[‡]Assistant Professor, Aerospace and Ocean Engineering Dep., Virginia Tech, Blacksburg, VA 24060
[§]Associate Professor, Dep. of Mechanical Engineering, Michigan Tech, Houghton, MI 49931
[¶]Associate Professor, Dep. of Mechanical Engineering, Michigan Tech, Houghton, MI 49931

Debye length, the more charge is needed to generate the same force. This limitation factor will be taken into consideration when using Coulomb forces in a wide range of altitudes.

The applications for this type of study can range anywhere from spacecraft docking maneuvers to large formation keeping. Therefore, an objective of this paper is to determine how to size various differential perturbations and determine their effects on the relative motion of satellites for a broad range of applications. To achieve this, perturbation effects are explored at altitudes from LEO to GEO and separation distances ranging from 10 to 1000 meters. The plasma Debye lengths are investigated for Coulomb formation flying application for LEO to GEO altitudes. The perturbation accelerations considered are the effects due to differential $J_2$ through $J_6$, atmospheric drag, and solar radiation pressure. The relative accelerations due to these perturbations are calculated within this range to get a measure of the forces needed to compensate for them. What we might expect to see is a domination of the atmospheric drag forces in lower earth orbit, and then either $J_2$ or solar radiation pressure becoming dominant at higher altitudes. This is then taken one step further and the charges necessary to generate these forces are also calculated. This allows us to explore the effects of multiple spacecraft charging and Debye length. However, the overall goal of this paper is to size these accelerations and associated voltage levels to explore the feasibility of missions that would take advantage of Coulomb forces in this manner. Two types of Coulomb formation flying are considered. The first mission types are classical bounded Hill frame formation where the spacecraft charges are used to compensate for the differential perturbations. Note that in this scenario all spacecraft are able to interact with each other. The second mission scenario introduces the concept of a "gluon" chief spacecraft. This craft is designed specifically to charge to very high levels, thus reducing the deputy charge requirements. As a result, the deputy electrostatic fields are assumed to not interact with each other. Numerical studies illustrate the required maintenance spacecraft voltage level to compensate for different types of differential perturbations.

## PLASMA PARAMETERS CONCERNING COULOMB THRUSTING

The concept of Debye shielding is fundamental to plasma physics. Qualitatively, Debye shielding can be viewed as a screening process whereby the mobile charges in a plasma screen out, or spatially neutralize an immersed test charge. For instance, consider placing a positive point charge within a plasma. The plasma particles, which exist in a gaseous state, are mobile and will respond to the presence of the charge: the positive test charge will attract a neighboring cloud of negative charges while creating a local void of positive charges in its vicinity. When averaged over some region in space centered on the test charge, the net charge within the specified volume will be zero. As a result, another test charge placed a long way from this volume will see a cloud with zero net charge and will thus experience very little electrostatic force from the test charge.

In order to perform Coulomb thrusting between spacecraft it is necessary that the plasma Debye length be greater than (or at least on the order of) the inter-spacecraft separation. This precludes the use of Coulomb control in cold, high-density plasmas such as that found in the ionosphere environment of LEO orbits. A qualitative depiction of the magnetosphere plasma environment is shown in Figure 1, where the diagonal lines represent constant values of Debye length with plasma density and temperature indicated on the axes. For approximate values, the Heidelberg Dust Research group has compiled a convenient set of representative plasma parameters[1] that are repeated in Table 1.

It is apparent from Figure 1 and Table 1 that the only feasible regime for inter- spacecraft Coulomb thrusting with contemporary-sized vehicles is the outer magnetosphere/GEO orbital environment. The centimeter-scale Debye lengths inside the plasmasphere render electrostatic interaction between vehicles negligible except at very small separation distances.

---

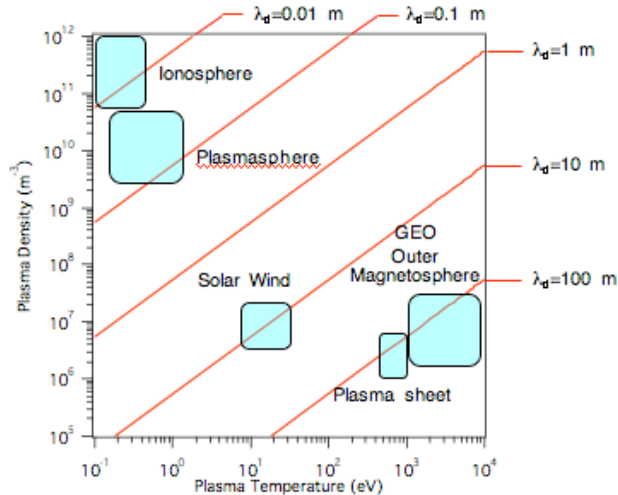[1] http://www.mpi-hd.mpg.de/dustgroup/~graps/earth/magnetosphere.html

Figure 1. Plasma regimes of the Earths magnetosphere. Red diagonal lines indicate constant values of Debye length.

Table 1. Plasma properties in the vicinity of Earth

| Region | Altitude | Density $(m^{-3})$ | Temperature (eV) | Debye Length (m) |
|---|---|---|---|---|
| Ionosphere | 1 $R_e$ | $10^{11}$–$10^{12}$ | 0.02–0.2 | 0.01–0.03 |
| Plasmasphere[4] | 1–5 $R_e$ | $10^{9}$–$10^{10}$ | 0.2–1.2 | 0.03–0.26 |
| GEO/Outer Mangetosphere[5] | 5–10 $R_e$ | $5 \cdot 10^5$–$10^7$ | 1,000–3,000 | 75–575 |
| Plasmasheet Magnetotail[4] | 10–15 $R_e$ sunward 10–100's $R_e$ anti-sunward | $5 \cdot 10^5$–$8 \cdot 10^5$ | 1,700–25,000 | 340–1,600 |
| Solar Wind[6] | Outside magnetosphere | $3 \cdot 10^6$–$9 \cdot 10^6$ | 10–100 | 8–43 |

## ORBITAL DISTURBANCES OF SPACECRAFT CLUSTERS

This section discusses the expected disturbance levels that a cluster of spacecraft will experience. The orbit altitudes will range from Low Earth Orbit (LEO) to Geostationary Earth Orbits (GEO), while the spacecraft separation distances vary between 10 and 1000 meters. In particular, the *worst case* accelerations relative to the spacecraft cluster/formation center of mass are of interest. This information will then be used to determine minimum required maintenance charge/voltage levels to be able to compensate for these disturbances.

### Relative Acceleration Magnitudes

To study the relative motion of spacecraft in nearly circular orbits, the Clohessy-Wiltshire-Hill equations are commonly used.[7,8,9] These equations linearize the relative motion dynamics with respect to a *constantly* rotating reference frame. They have a well-known analytical solution to the unperturbed motion which decouples the in-plane and out of orbit plane motions. The CW equations are very convenient to develop rendezvous and near-circular formation flying control laws.[10,11] With traditional spacecraft formation flying concepts, each craft contains its own inertial propulsion system, typically a high efficiency ion engine. As relative motion errors are detected, the thruster is used to correct the motion with respect to the rotating Hill frame.

However, the Coulomb thrusting concept acts very differently. Here the spacecraft push and pull off each other to control the relative motion. The inertial orbit of the cluster is of secondary importance compared to the formation shape and is not compensated for with Coulomb thrusting. Thus, to determine the necessary relative orbit maintenance charge/voltage levels to compensate for differential perturbations, it is essential that the drift of the formation center of mass (Hill frame origin) is taken into account.
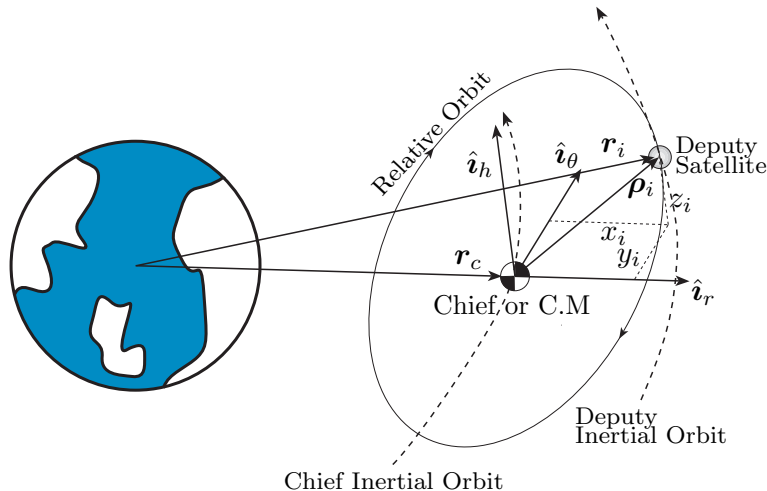


Figure 2. Diagram of the Relative Motion Problem

In order to avoid the linearization and constant orbit rate issues of the CW equations, we have chosen to use a full non-linear simulation of the spacecraft with the perturbations included as inertial acceleration vectors. Figure 2 describes the set-up of the relative motion problem and the notation to be used in the rest of this report. Let there be $N$ charged spacecraft present. The inertial position vectors of the satellites is given by $\boldsymbol{r}_i$, while

$$\boldsymbol{r_c} = \frac{1}{M} \sum_{i=1}^{N} m_i \boldsymbol{r}_i \qquad (1)$$

is the formation inertial center of mass vector. Here $M$ is the total system mass and $m_i$ is the mass of the $i_{th}$ spacecraft.

The Hill frame unit direction vectors $\mathcal{H} : \{\hat{\boldsymbol{i}}_r, \hat{\boldsymbol{i}}_\theta, \hat{\boldsymbol{i}}_h\}$ are defined through:

$$\hat{\boldsymbol{i}}_r = \frac{\boldsymbol{r_c}}{r_c} \qquad \hat{\boldsymbol{i}}_\theta = \hat{\boldsymbol{i}}_h \times \hat{\boldsymbol{i}}_r \qquad \hat{\boldsymbol{i}}_h = \frac{\boldsymbol{r_c} \times \dot{\boldsymbol{r}}_c}{|\boldsymbol{r_c} \times \dot{\boldsymbol{r}}_c|}$$

In the CW equations, this frame is treated as having a constant rotation rate. However, in this differential disturbance study the actual $\dot{\boldsymbol{r}}_c$ is taken into account. The rotation matrix $[HN]$, which will rotate vector components taken with respect to the inertial frame to vector components taken with respect to the the Hill frame, is defined as

$$[HN] = \begin{bmatrix} \hat{\boldsymbol{i}}_r & \hat{\boldsymbol{i}}_\theta & \hat{\boldsymbol{i}}_h \end{bmatrix}^T \qquad (2)$$

Defining the relative position vector as $\boldsymbol{\rho}_i = \boldsymbol{r}_i - \boldsymbol{r_c}$, this vector can be mapped between inertial and Hill frame vector components using $^{\mathcal{H}}\boldsymbol{\rho}_i = [HN] \, ^{\mathcal{N}}\boldsymbol{\rho}_i$.

The inertial equations of motion of a satellite are given by

$$\ddot{\boldsymbol{r}}_i = -\frac{\mu}{r_i{}^3} \boldsymbol{r}_i + \boldsymbol{a}_{d_i} \qquad (3)$$

4

where $\boldsymbol{a}_{d_i}$ is the disturbance acceleration acting on the $i^{\text{th}}$ satellite. Of interest is how this disturbance acceleration will influence the motion of the satellite relative to the formation/cluster center of mass $\boldsymbol{r}_c$. In particular, we take into account here that $\boldsymbol{r}_c$ itself will also be influenced by the disturbance. For example, if both satellites are experiencing the same atmospheric drag, then the differential disturbance would be zero because the center of mass is being disturbed by the same amount as the satellites. Similarly, if one satellite has twice the disturbance drag acceleration compared to the 2nd craft, then each craft would only have to compensate for half of this drag (assuming equal masses).

Equation (3) is used to perform the numerical simulations. Any Hill-frame specific initial conditions are first mapped into the inertial frame to start the simulation. The inertial acceleration is written as

$$\ddot{\boldsymbol{r}}_i = \ddot{\boldsymbol{r}}_c + \ddot{\boldsymbol{\rho}}_i \tag{4}$$

Next, let $\ddot{\hat{\boldsymbol{\rho}}}_i$ be the inertial relative acceleration if no disturbance accelerations are present (Keplerian motion case).

$$\ddot{\hat{\boldsymbol{\rho}}}_i = \ddot{\hat{\boldsymbol{r}}}_i - \ddot{\hat{\boldsymbol{r}}}_c \tag{5}$$

Here $\ddot{\hat{\boldsymbol{r}}}_i$ and $\ddot{\hat{\boldsymbol{r}}}_c$ are defined as follows:

$$\ddot{\hat{\boldsymbol{r}}}_i = -\frac{\mu}{r_i{}^3}\boldsymbol{r}_i \tag{6}$$

$$\ddot{\hat{\boldsymbol{r}}}_c = \frac{1}{M}\sum_{i=1}^{N} m_i \ddot{\hat{\boldsymbol{r}}}_i \tag{7}$$

Thus the ^ quantities are the unperturbed accelerations of the Keplerian relative motion case. Using Eq. (3) to integrate the satellite inertial position vectors, at any instant of time the $\boldsymbol{r}_i(t)$ will be available during post-processing, and these local "unperturbed" states can be computed.

Next, the relative inertial acceleration can be written as $\ddot{\boldsymbol{\rho}}_i = \ddot{\hat{\boldsymbol{\rho}}}_i + \delta\ddot{\boldsymbol{\rho}}_i$ where we separate the naturally occurring relative acceleration from the relative acceleration due to the perturbation forces. Solving for the differential disturbance acceleration vector $\delta\ddot{\boldsymbol{\rho}}_i$ we find

$$\delta\ddot{\boldsymbol{\rho}}_i = \ddot{\boldsymbol{r}}_i - \ddot{\boldsymbol{r}}_c - \ddot{\hat{\boldsymbol{\rho}}}_i \tag{8}$$

To be able to maintain a cluster or formation of charged spacecraft, the spacecraft charging capabilities must be large enough to be able to compensate for the worst case differential disturbance acceleration $\delta\ddot{\boldsymbol{\rho}}_i$ which will be encountered for a particular orbit altitude and formation size. With each orbital disturbance type the differential disturbance acceleration is computed. These worst case disturbance acceleration values are then used in the next section to compute required minimum spacecraft charge/voltage levels to compensate for this disturbance.

### Differential Gravitational Zonal Harmonics

The $J_2$ through $J_6$ perturbations arise from the fact that the Earth is not a perfect sphere, but rather ellipsoidal in shape. Of these gravitational disturbances, the 2$^{\text{nd}}$ order zonal harmonic, called the $J_2$ term, is about three orders of magnitude larger than the remaining harmonics. It provides the dominant formation flying perturbation for spacecraft of equal type and build.[12] These formation flying spacecraft are typically envisioned to be flying about 1 km apart, or further.[13] However, for the Coulomb thrusting concept study, much smaller separation distances are considered. With these smaller separation distances the differential $J_2$ influence will become ever smaller. Of interest is how these differential accelerations compare to other orbital perturbations such as differential atmospheric drag and differential solar radiation pressure.

The inertial disturbance acceleration vector due to $J_2$ through $J_6$ can be modelled as direct functions of inertial position and the first six zonal harmonics. However, only the first zonal harmonic has a significant contribution for this study and is expressed as.[9]

$$\boldsymbol{a}_{J_2} = \frac{-3}{2} J_2 \left(\frac{\mu}{r^2}\right) \left(\frac{r_{\text{eq}}}{r}\right)^2 \begin{pmatrix} \left(1 - 5\left(\frac{Z}{r}\right)^2\right)\frac{X}{r} \\ \left(1 - 5\left(\frac{Z}{r}\right)^2\right)\frac{Y}{r} \\ \left(3 - 5\left(\frac{Z}{r}\right)^2\right)\frac{Z}{r} \end{pmatrix} \tag{9}$$

Here $r_{\text{eq}}$ is the equatorial radius of the Earth and $\mu$ is the gravitational constant of the Earth. The variables $X$, $Y$, and $Z$ are the position coordinates with respect to the ECI (Earth Centered Inertial) frame and the orbit radius is $r = \sqrt{X^2 + Y^2 + Z^2}$.

The magnitude of the $J_2$ induced relative motion disturbance depends on how the relative orbit is formed (wether the out-of-plane motion is achieved through inclination or ascending node differences), and on the location (anomaly angle) within the orbit.[14,9,15] This study is based on investigating worst case scenarios to determine minimum spacecraft charge sizing requirements. The radar interferometry problem was of particular interest to this project. Here the desired relative orbits have circular projections relative to the local horizontal plane ($\hat{\boldsymbol{i}}_\theta$–$\hat{\boldsymbol{i}}_h$ plane). Let a relative position vector be written using Hill frame vector components as

$$\boldsymbol{\rho} = x\hat{\boldsymbol{i}}_r + y\hat{\boldsymbol{i}}_\theta + z\hat{\boldsymbol{i}}_h \tag{10}$$

The analytical solution to the CW equations shows that all bounded relative orbits with a circular chief must satisfy:[8,9]

$$x(t) = A_0 \cos(nt + \alpha) \tag{11}$$
$$y(t) = -2A_0 \sin(nt + \alpha) \tag{12}$$
$$z(t) = B_0 \cos(nt + \beta) \tag{13}$$

where $A_0$ and $B_0$ are relative orbit amplitudes, while $\alpha$ and $\beta$ are phase angles of the relative motion. The parameter $n = \sqrt{\mu/r_c^3}$ is the chief's mean orbit rate. To achieve the circular projection of the relative motion in the local horizontal plane, the initial orbit must be setup such that $B_0 = 2A_0$, and either $\alpha = \beta$ or $\alpha = \beta + \pi$.[9] To determine the worst case differential $J_2$ accelerations, a quick study is preformed where the phase $\alpha$ is swept across all possible values. All orbits are initialized as they cross the equator. When $\alpha$ is initially either 90 or 270 degrees produces a slightly larger acceleration compared to any other initial angle over an orbit period. Thus, to determine the worst case differential $J_2$ disturbance acceleration, these initial conditions are used to setup two satellites and then integrate the inertial equations of motion for one orbit. The worst differential acceleration is then recorded for the particular orbit altitude and relative orbit size.

Figure 3 illustrates the maximum differential $J_2$ accelerations in units of $\log_{10}(\text{m/s}^2)$. The altitude (horizontal axis) is swept form LEO (300 to 1000 km) to GEO (35,000 km). The separation distances (the $A_0$ parameter in Eq. (11)) is swept from $10 - 1000$ meters. The chief orbit is initially set to be a circle in each case. The coutour plots illustrate the resulting maximum differential $J_2$ induced accelerations that were encountered. Three cases are illustrated for chief inclination angles of 0, 45 and 90 degrees. As expected, the differential $J_2$ perturbations increase with increasing formation size and with decreasing orbit altitude. As the orbit inclinations are increased, the resulting worst cases differential accelerations increase slightly, but not substantially.

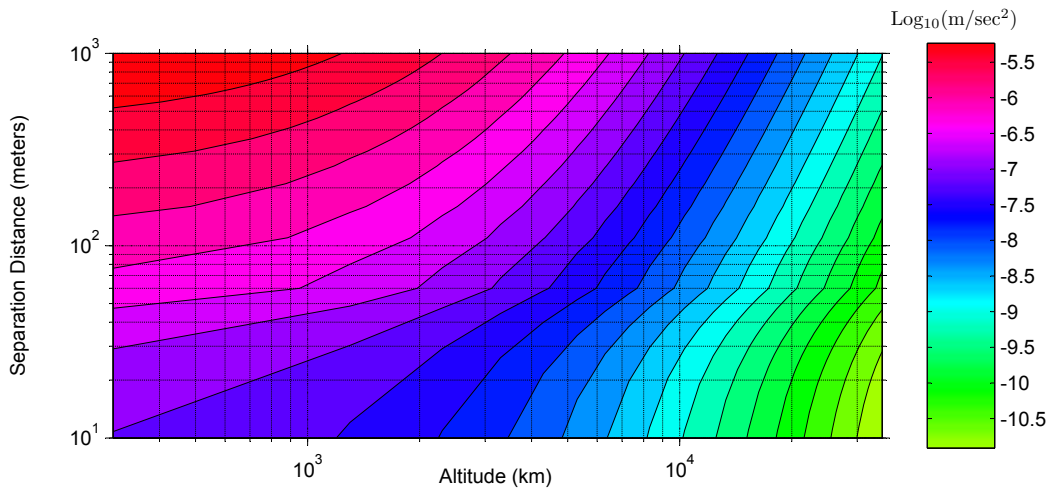### Differential Atmospheric Perturbations

The next perturbation to examine is the drag force due to the atmosphere. This effect will be dominant in the low earth orbit altitudes and become negligible at higher altitudes. The magnitude
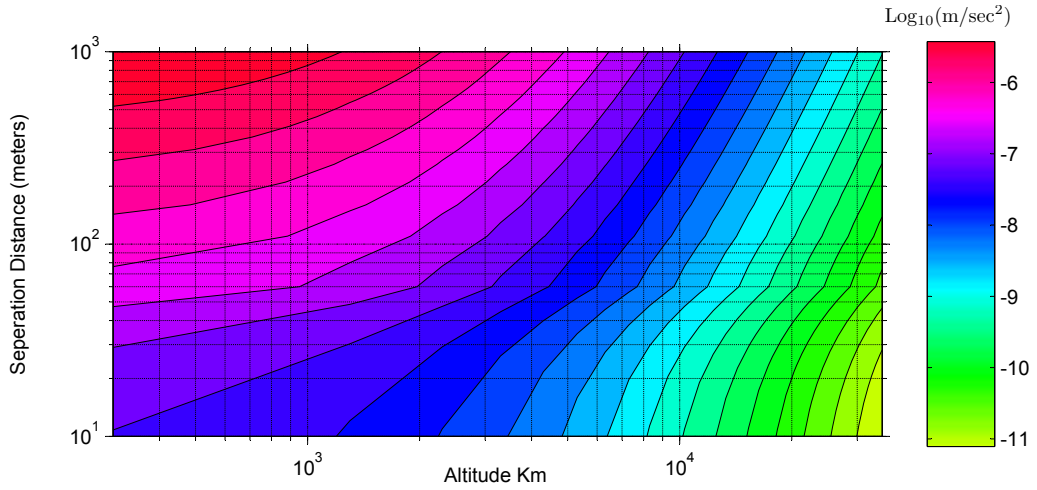
(a) $\log_{10}$ of Max Acceleration due to $J_2$ trough $J_6$ with $i = 0^{\circ}$
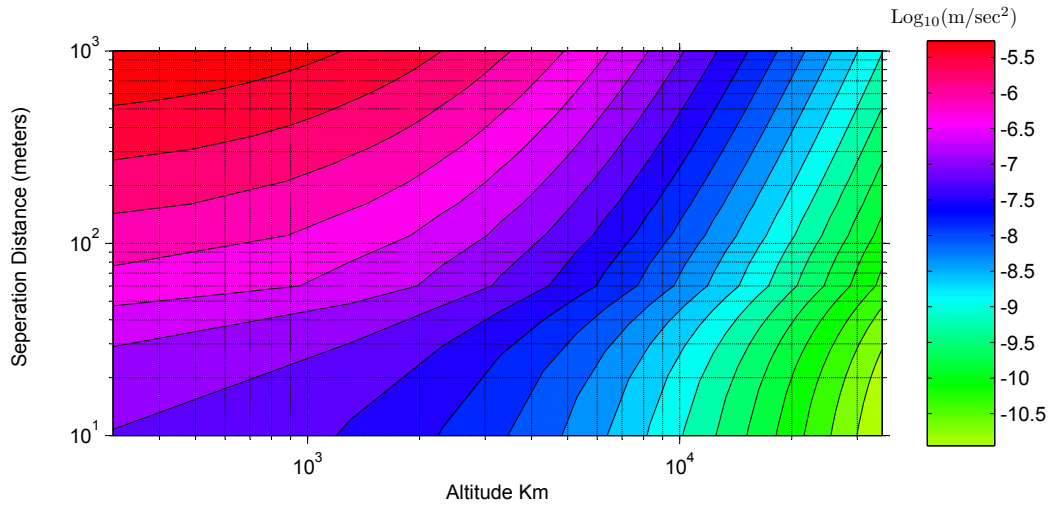


(b) $\log_{10}$ of Max Acceleration due to $J_2$ trough $J_6$ with $i = 45^{\circ}$



(c) $\log_{10}$ of Max Acceleration due to $J_2$ trough $J_6$ with $i = 90^{\circ}$

Figure 3. Contour Plots of Acceleration in $\log_{10}(\text{m/s}^2)$ vs. Separation Distance and Altitude for $J_2$ through $J_6$ Perturbations
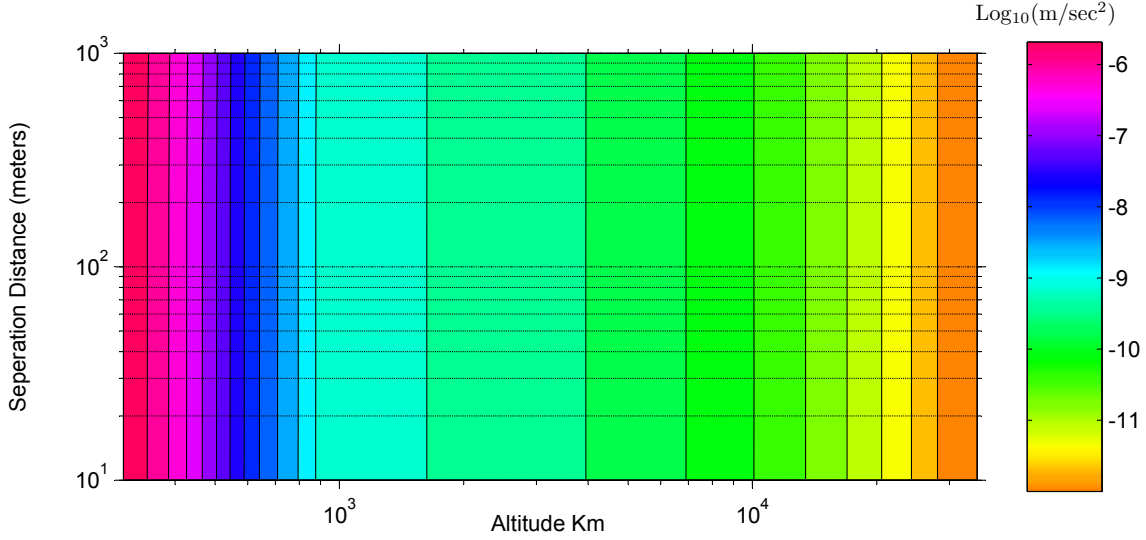
Figure 4. Contour Plots of Differential Atmospheric Drag Acceleration in $\log_{10}(\text{m/s}^2)$ vs. Separation Distance and Altitude

of acceleration due to atmospheric drag is modeled as.[9]

$$a_D = -\frac{1}{2}\rho(C_d A/m)V^2 \tag{14}$$

Here $\rho$ is the atmospheric density, $C_D$ is the coefficient of drag, $A$ is the satellite's cross-sectional area, and $V$ is the current inertial velocity of the spacecraft. The drag force acts in the opposite direction of velocity:[9]

$$\boldsymbol{a}_{d_i} = a_{d_i}\hat{\boldsymbol{i}}_v = a_{d_i}\frac{\dot{\boldsymbol{r}_i}}{|\dot{\boldsymbol{r}_i}|} \tag{15}$$

The atmospheric density model used is the United States Standard Atmosphere Model from 1976. The actual model contains density data for altitudes ranging from 86 to 1000 km. Above this range it is assumed that density becomes very close to zero and the drag force is non-existent.[16]

The next two variables to model in Eq. 14 are the coefficient of drag $C_d$ and the cross-sectional area $A$. For the purpose of sizing the value of $C_d$, a general cylindrical shape is considered for the spacecraft rather than the previous spherical model. If spherical spacecraft of equal mass are considered, then the differential atmospheric draft would be trivially zero. However, in the cylindrical spacecraft case the attitude of the spacecraft will have an influence on the $C_d$ value. This aspect allows us to study differential drag for two or more satellites in a formation. The next step is to estimate the value for $C_d$ for worst and best case scenarios based on exsiting data on an actual spacecraft. In Reference 17 there is one specific craft, Intercosmos-16, which is a scientific spacecraft with a cylindrical shape and no solar panels. The data table on its drag properties has a $C_d$ for maximum cross-sectional area of 2.67 and for minimum cross-sectional area that value drops to 2.1. This data gives us a sufficient range of $C_d$ values to use in our study of differential drag on a formation of satellites. For our differential atmospheric drag simulations we chose the typical craft configurations with a mass of 50 kg craft, while the radius is 0.5 meters and a height equal to three times the radius. This provides our numerical simulation with realistic spacecraft parameters to study a worst case scenario for differential drag forces on relative motion.

Figure 4 illustrates the computed differential atmospheric drag accelerations for LEO to GEO orbit, with the separation distances ranging from 10–1000 meters. Because all satellites are essentially in circular orbits (as seen by inertial frame), the inertial velocity is essentially constant here. Thus, the differential atmospheric disturbance will not depend on the spacecraft separation distance. Rather, it only depends on the orbit altitude. Note that the Standard atmosphere model used only provided data up to a height of 1000 meters. Beyond that the atmosphere is modeled to simply decay to zero exponentially.

**Differential Solar Radiation Pressure**

Solar radiation drag is created by having the sun's light reflect off the spacecraft. Through momentum conservation, a small force is exerted onto the craft. The magnitude of this force depends on the apparent size and reflectivity of the spacecraft. To model the solar radiation pressure we will use a spherical spacecraft model. The equation for this model is shown below:[18]

$$\boldsymbol{a}_R = -C_R \frac{A\Phi\boldsymbol{R}}{mcR^3} \tag{16}$$

Where $A$ is the cross-sectional area facing the sun, and $\Phi$ is the solar constant. Also, $m$ is the spacecraft mass, $c$ is the speed of light, and $C_R$ is the pressure radiation coefficient. Lastly, the vector $\boldsymbol{R}$ is the inertial vector pointing from the sun to the planet you are orbiting in AU, while $R$ is simply its magnitude. In this part of the equation, it is assumed that there is a quadratic drop in radiation pressure as you increase your distance past 1 AU, which is the distance from the Earth to the Sun. Without loss of generality, for our simulation we will choose a vector in vernal equinox direction. The motion of all satellites considered is insignificant here compared to the size of the Earth/Sun inertial position vector.

The other variables in the equation are simply constants. For cross-sectional area $A$ and mass $m$, the same values are used as for the atmospheric drag force calculation. The pressure radiation coefficient is taken to be $C_R = 1.3$ from the average value based on recent data.[18] The solar constant $\Phi$ is 1372.5398 W/m$^2$ and the speed of light is $c =$2.997 m/s. The worst case differential solar radiation drag is found to be about $10^{-7.5}$ m/s$^2$. This value is the same for different orbit altitudes and spacecraft separation distances.

**Overview of Dominant Perturbations Zones**

The previous three sections discussed the differential perturbations due to $J_2$ perturbations, atmospheric drag, as well as solar radiation drag. In all cases the craft are assumed to have a mass of $m = 50$ kg, and a nominal radius of 0.5 meter. Figure 5 provides an overview of altitude and separation distance zones showing which perturbation is the most significant for a particular zone. Traditional formation flying applications treat the $J_2$ perturbation as the dominant disturbance of the formation geometry.[19, 20, 21] Here the craft are assumed to be of equal type and build. However, even if all craft have the same shape, different orientations can cause significant differential atmospheric drag in LEO regimes. Figure 5 shows that for conditions used in this study, the differential atmospheric drag will dominate at LEO up to separation distances of 350 meters. As the orbit altitude is increased to about 500 km, the differential atmospheric drag dominant zones vanish. For large separation distances at LEO the differential $J_2$ perturbation becomes dominant, even if differential spacecraft attitudes are considered. This tendency is expected because the differential $J_2$ perturbation increases with separation distance, while the differential atmospheric drag does not.

As the considered orbit altitudes are increased to Medium Earth Orbits (MEO) and geostationary orbits (GEO), the differential $J_2$ perturbation is decreased. The further away from Earth the spacecraft is, the more the Earth's gravitational potential begins to resemble that of a point-mass. Past an altitude of 2000 km, the differential solar radiation pressure starts to become the dominant
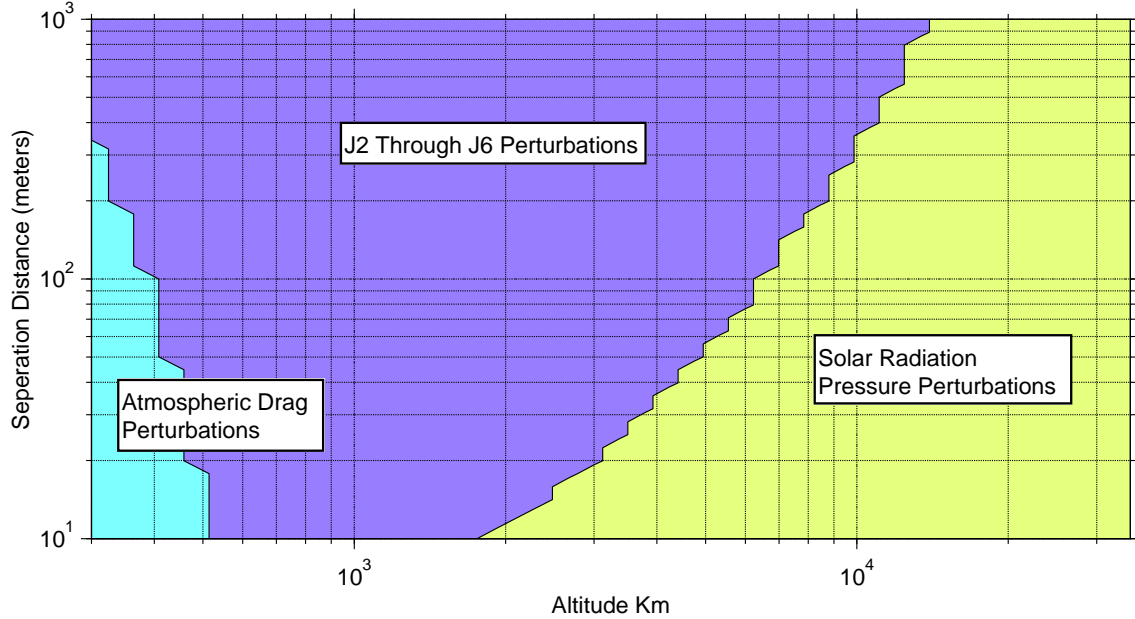
Figure 5. Dominant Differential Perturbation Zones Illustration.

perturbation at low separation distances. At high Earth orbit regions above 10,000 km, which will typically be considered in this study for charged spacecraft missions, the differential solar radiation pressure is the largest perturbation even out to 1000 meter separation distances.

**Earth Magnetic Lorentz Force**

Lastly we want to explore the effects of Earth's magnetic field on our spacecraft. Because we will be generating a significant amount of charge or voltage to compensate for these orbital disturbances, that charge will in turn create an acceleration due to Earth's magnetic field. This acceleration or force is known as the Lorentz Force and is written in equation 17 from basic physics.

$$\boldsymbol{F} = q\,\dot{\boldsymbol{r}} \times \boldsymbol{B} \tag{17}$$

In this equation $q$ is the charge generated by the craft in Coulombs, $\dot{\boldsymbol{r}}$ is the inertial velocity vector of the spacecraft in m/s, and $\boldsymbol{B}$ is the inertial magnetic field vector of the Earth in units of Tesla. The Earth's magnetic field generally resembles the field around a magnetized sphere, or a tilted dipole. As of 1999, the dipole axis was tilted approximately 11.5º from the spin axis, and drifting approximately 0.2º/yr. Its strength at the Earths surface varies from approximately 30000nT near the equator to 60000nT near the poles. Further, there exists a low magnetic intensity field at approximately 25º S and 45º W known as the Brazilian Anomaly. A high exists at 10º N and 100º E, and the two of these together suggest that not only is the dipole axis tilted, but it does not quite pass through the center of the Earth.[22] The accepted model for Earth's magnetic field is the International Geomagnetic Reference Field, put forth by the International Association of Geomagnetism and Aeronomy (IAGA). An overview of this model can be found on the website of the IAGAs Working Group V-MOD.[2]

For a reference case, we pick a longitude of about -100 degrees and a latitude of 10 degrees, the Brazilian Anomaly. As the orbit altitude is swept, the magnetic field strength is computed

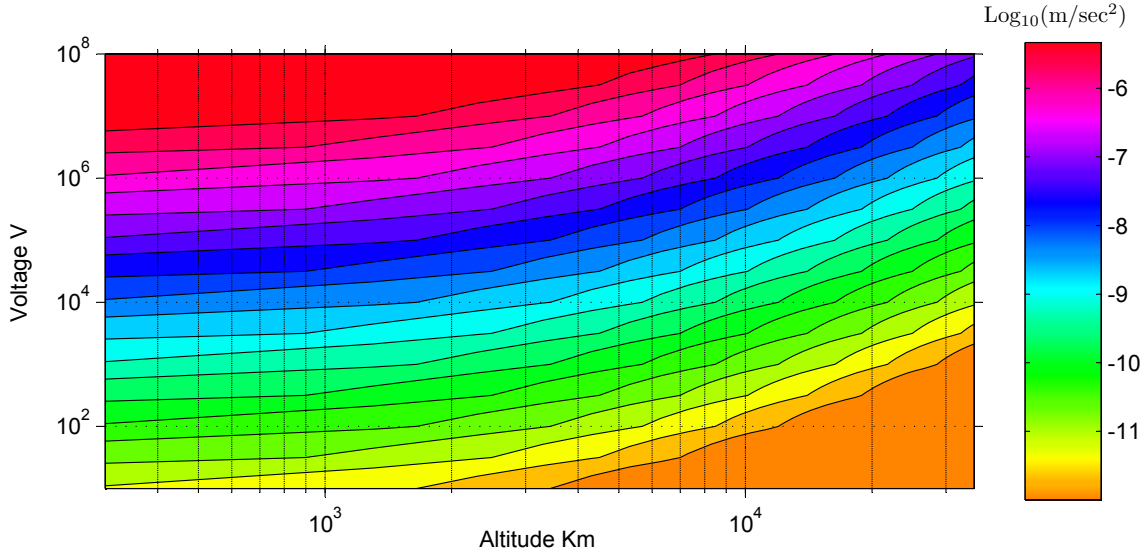---

[2]http://www.ngdc.noaa.gov/IAGA/vmod/igrf.html

Figure 6. Contour Plots of Acceleration in $\log_{10}(\text{m/s}^2)$ vs. Voltage and Altitude over the 10º N and 100º E Location.

for altitudes over this location to determine worst case conditions. The velocity vector $\dot{\boldsymbol{r}}$ is to be taken as the circular velocity at the given altitude. Lastly, the voltage of the spacecraft and the orbit altitude are swept. The altitude range will be the same as for the previous disturbance acceleration cases. The voltage will be swept from $10^1$ to $10^8$ volts in order to supply force data for a broad range of voltages. The Lorentz acceleration for a 50 kg craft is then plotted in Figure 6. From the figure we can see that for reasonable voltages on the order of kilovolts to hundreds of kilovolts, the spacecraft will experience accelerations about two orders of magnitude below the expected disturbance accelerations due to the perturbations. This suggests that even though this force is small, it is still there and must be considered in higher fidelity simulations. Also notice that the accelerations become relatively high when the voltage increases to $10^8$ volts, even higher than the disturbance accelerations. This can become a factor if the craft are relatively far apart and a much higher voltage is needed to compensate for a disturbance.

## REQUIRED SPACECRAFT CHARGE LEVELS

This section investigates the minimum required spacecraft charge levels necessary to compensate for the differential orbital perturbations. Any feedback charge control strategy would require at least this charge level to compensate for the disturbances, and additional charge to perform orbit corrections.

### Spacecraft Voltage Computation

The charges $q_i$ are the physical quantities which determine the Coulomb force magnitude.[23] However, when implementing such spacecraft charges, the technical concern will be the charge density (voltage) across the craft. The higher the voltage, the more challenging it will be to implement any charge control law. Thus, this study evaluates what the necessary spacecraft voltages/charge levels are to compensate for differential orbital perturbations. Note that the Coulomb forces are not sized here to compensate for the total orbital perturbation. In fact, it is impossible to change the inertial momentum of the charged satellite cluster using internal Coulomb forces. Rather, the Coulomb
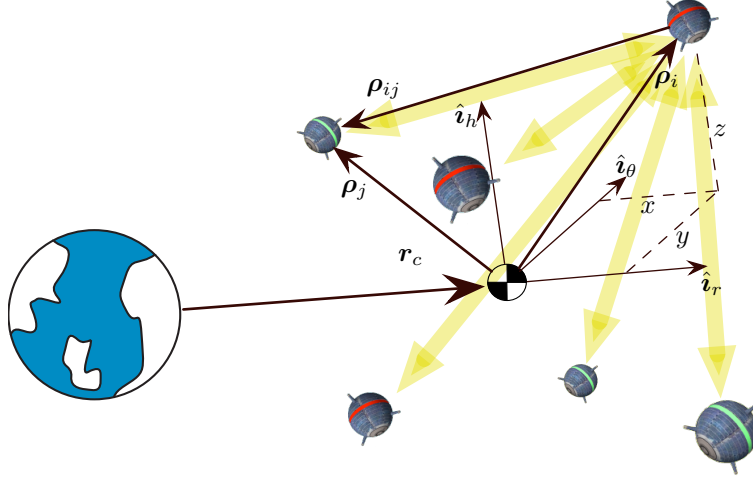
Figure 7. Coulomb Spacecraft Formation Illustration

forces are sized such that they will be able to compensate for the differential perturbations which would cause the formation to change shape, size or orientation.

Unless noted otherwise, the typical spacecraft is assumed to be spherical in shape, have a radius of $r = 0.5$ meters, and a mass of $m = 50$ kg. The differential perturbation levels are taken from the conservative worst case results discussed in the previous section. Once a required spacecraft charge $q_i$ is computed, then the equivalent spacecraft voltage is evaluated using

$$V_i = k_c \frac{q_i}{r} \tag{18}$$

where $k_c$ is the Coulomb's constant. This formula assumes the charge is homogeneously distributed across a sphere of radius $r$. How to compute the required spacecraft charge $q_i$ levels depends on the mission scenario being considered.

### Free-Flying Formation Concept

*Formation Description*

Let us first consider a mission scenario where all charged spacecraft are flying within each others electrostatic spheres of influences. The spacecraft formation is designed such that the nominal geometry are control-free solutions of the relative equations of motion. Any formation flying errors relative to the formation center of mass will then be controlled using the electrostatic (Coulomb) forces. For example, consider the typical formation flying configuration where all the satellites are flying in bounded elliptical relative orbits with circular projections in the local horizontal plane. If the relative orbit dimension is reduced to dozens to hundreds of meters, then the electrostatic field of one satellite will influence the motion of all other craft within this formation. In this scenario a single craft is able to interact with all other formation craft to produce the required Coulomb force. Let $n = \sqrt{\mu/a^3}$ be the mean orbital rate of the circular chief motion, then the CW equations are given by:[7,8,9]

$$\ddot{x} - 2n\dot{y} - 3n^2 x = \alpha_x \tag{19a}$$
$$\ddot{y} + 2n\dot{x} = \alpha_y \tag{19b}$$
$$\ddot{z} + n^2 z = \alpha_z \tag{19c}$$

12

If only Coulomb forces are perturbing the Keplerian orbital motion, then the disturbance acceleration vector $\boldsymbol{\alpha}$ is given by

$$\boldsymbol{\alpha} = {}^{\mathcal{H}}\begin{pmatrix} \alpha_x \\ \alpha_y \\ \alpha_z \end{pmatrix} = -\frac{k_c}{m_i} \sum_{j=1, j\neq i}^{N} \frac{q_i q_j}{\rho_{ij}^3} \boldsymbol{\rho}_{ij} e^{-\frac{\rho_{ij}}{\lambda_d}} \tag{20}$$

where $\boldsymbol{\rho}_{ij} = \boldsymbol{\rho}_j - \boldsymbol{\rho}_i$. The purpose of this study is to investigate necessary spacecraft charge levels to compensate for differential orbital perturbations. The nominal formation geometry is assumed to be a control free solution. Analytical solutions to the CW equations are well known and have been applied to the formation flying problem.[24, 25, 26, 10] Control free solutions of relative orbits exploiting the mean $J_2$ perturbations are discussed in References 19, 23, 27. To size the minimum spacecraft charge level to *maintain* a formation shape, the magnitude of the local differential orbital perturbations must be considered. Note that any final feedback strategy would require charge levels higher than those discussed in this section.

*Minimum Maintenance Voltage Computation*

To compute the worst case spacecraft voltage to compensate for differential orbital perturbations, we study the disturbance accelerations acting on a single spacecraft within this formation over one orbit period. Assume the formation contains $N$ spacecraft of essentially equal type and build. Let us define the $L(N-1)$ dimensional vector charge product vector $\boldsymbol{Q}$ as

$$\boldsymbol{Q} = \begin{pmatrix} Q_{i1} & Q_{i2} & \cdots & Q_{ij} & \cdots & Q_{iN} \end{pmatrix}^T \tag{21}$$

with $i \neq j$ and where $Q_{ij} = q_i q_j$. The parameters $q_i$ and $q_j$ are the charge levels of the i$^{\text{th}}$ and j$^{\text{th}}$ spacecraft respectively. Further, let us define the $3 \times L$ matrix $[A(t)]$ as

$$[A(t)] = \begin{bmatrix} \frac{\boldsymbol{\rho}_{i1}}{\rho_{i1}^3} e^{-\frac{\rho_{i1}}{\lambda_d}} & \cdots & \frac{\boldsymbol{\rho}_{ij}}{\rho_{ij}^3} e^{-\frac{\rho_{ij}}{\lambda_d}} & \cdots & \frac{\boldsymbol{\rho}_{iN}}{\rho_{iN}^3} e^{-\frac{\rho_{iN}}{\lambda_d}} \end{bmatrix} \tag{22}$$

with $i \neq j$. Note that the space plasma influence of the electrostatic field generation has been included in this $[A(t)]$ definition as the exponential term, $e^{-\frac{\rho_{ij}}{\lambda_d}}$, where $\lambda_d$ is the Debye length. The actual control acceleration $\boldsymbol{\alpha}_i$ experienced by the $i^{\text{th}}$ spacecraft is

$$\boldsymbol{\alpha}_i = -\frac{k_c}{m_i}[A(t)]\boldsymbol{Q} \tag{23}$$

Thus, to compensate for the disturbance acceleration $\boldsymbol{a}_d$, we set it equal to the control acceleration and solve for the charge product vector $\boldsymbol{Q}$.

$$\boldsymbol{Q} = -\frac{m_i}{k_c}[A(t)]^\dagger \boldsymbol{a}_d \tag{24}$$

Note that this disturbance acceleration is computed relative to the *drifting* formation center of mass as outlined earlier. Using the pseudo-inverse of the rectangular matrix $[A(t)]$ provides the minimum norm solution of the charge product vector. The charge of the $i^{\text{th}}$ spacecraft whose relative motion is being control is computed using

$$q_i = \sqrt{\max(|Q_{ij}|)} \tag{25}$$

*Numerical Sweeps of Maintenance Voltage*

To parameterize a family of Coulomb formation, the following scenario is used. Keeping space-based radar interferometry missions in mind, the analytical solution to the CW equations in Eq. (11) are used to setup a Coulomb formation of $N$ craft. In particular, the circular projection condition

$B_0 = 2A_0$ and $\alpha = \beta$ is enforced to yield circular formations as seen by an Earth observer. The $N$ craft are spaced equally along the relative orbit. The constant separation angle is $\varphi = 2\pi/N$.

To determine the disturbance acceleration $\boldsymbol{a}_d$ on the $i^{\text{th}}$ craft, this craft is allowed to perform a complete orbit about the Earth. The $N - 1$ remaining satellites are held in equivalent relative orbit positions compared to this $i^{\text{th}}$ craft to maintain the constant separation angles $\varphi$. Thus, at any instance in this simulation, the formation geometry satisfies the linearized bounded motion conditions. As the craft of interest completes its orbit, the true inertial position vectors $\boldsymbol{r}_i$ computed for all craft to determine the differential perturbation accelerations relative to the drifting formation center of mass. For a given orbit size (determined through $A_0$) and orbit altitude), the corresponding maximum required voltage is recorded.

The expected mean Debye lengths at different orbit altitudes were discussed in an earlier section. The only regions which are found to be feasible for Coulomb spacecraft formation flying were orbit radii greater than about $6$ $R_e$ up to GEO altitudes. Inside this radius the Van Allen radiation belts, as well as the dense, cold plasma environments of LEO altitudes yielded extremely small Debye lengths of millimeters to centimeters. Outside the Van Allen radiation belts the Debye length were found to vary from 100 meters up to 500–1000 meters, depending on the solar activities.

To perform numerical sweeps of required spacecraft voltage levels to compensate for differential orbital perturbations, all simulations use a GEO altitude. At lower HEO altitudes the Debye lengths are found to be very similar to the GEO altitude Debye lengths. Thus, numerical sweeps are performed where the Debye length is varied, as well as the formation size. At HEO altitudes the differential atmospheric disturbance are negligible. While the differential solar radiation pressure is the largest, the differential $J_2$ perturbations were included in these sweeps as well. Figure 8 illustrates contour plots of the resulting required spacecraft voltages. The results show that for separation distance of dozens of meters, the required voltages for the 0.5 meter radius craft is in the 10's of kilovolt level. To compensate for the separation distances of 100's of meters, the required voltage quickly increase into 100's of kilovolt levels. And lastly, the Debye length effect will cause the voltage levels to spike even higher at these separation distances to the hundred thousand's of kilovolts.

**Gluon Spacecraft Concept**

*Formation Description*

Next we discuss a satellite formation in which there is a massive satellite in the center, called a gluon. The deputy satellites are assumed to be in a bounded relative orbit around the Gluon or chief satellite. The main idea behind this type of formation is to have a dedicated gluon which can charge up to very high values. As a result, the deputy satellites can achieve a given inter-satellite control force using a much smaller charge level. The gluon is also much heavier and larger in size than the deputy. Because the deputy charge levels are relatively small, their mutual interactions can be neglected for $1^{\text{st}}$ order control studies. This contrasts with the very coupled and complex dynamics of the previously discussed Coulomb formations.

In order to accommodate high charge and still stay within an acceptable level of voltage, the gluon will have a large surface area. Due to the significant difference in mass and surface area between the gluon and deputy satellite, the solar drag, $J_2$ effect and atmospheric drag experienced by them will be different. In this section we study the effect of this differential drag and differential $J_2$ effect, and find the approximate magnitude of Coulomb force needed to compensate for this drag.

*Gluon Spacecraft Layout*

For this study, we consider only one deputy satellite and gluon. The gluon has a constant core mass and a large shell, supported by 8 thin cylindrical columns. The large shell helps in distributing the charge, thus reducing the voltage. The shell and its support structure are assumed to be made of
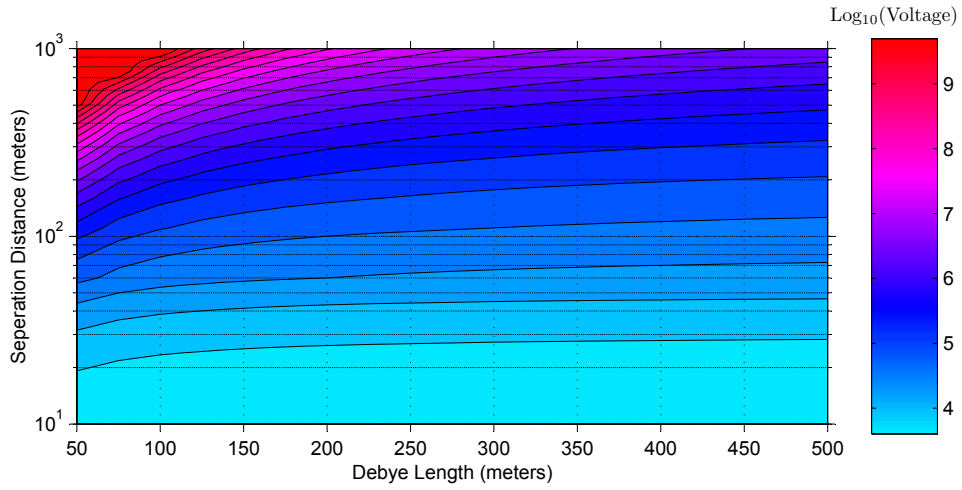
(a) $\log_{10}$ of Voltage for 2 Spacecraft
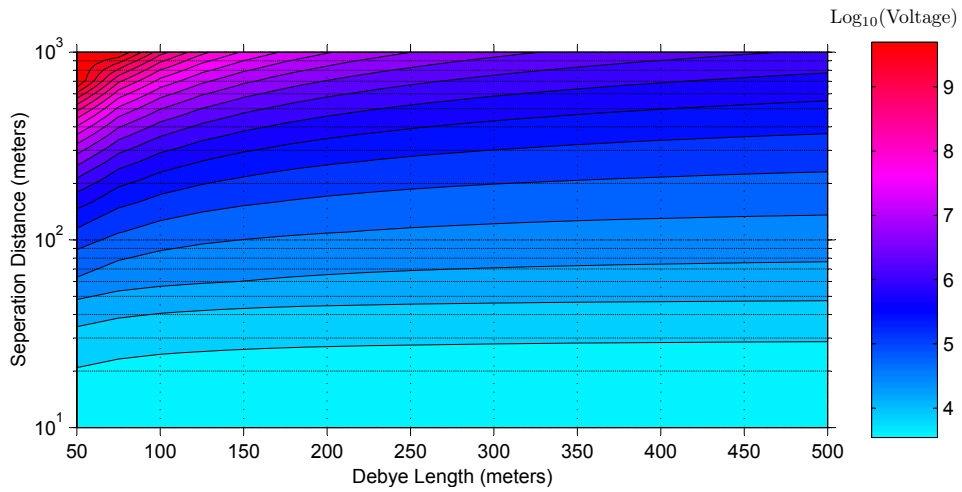


(b) $\log_{10}$ of Voltage for 4 Spacecraft
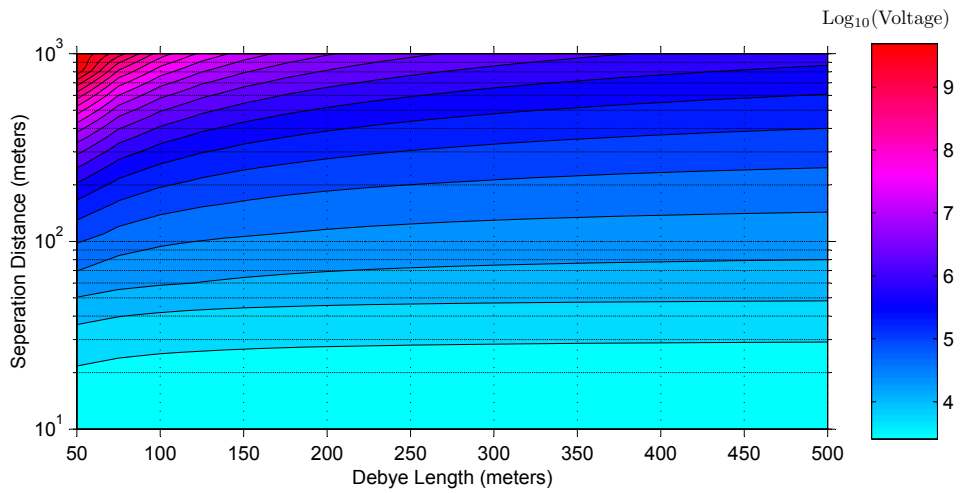


(c) $\log_{10}$ of Voltage for 5 Spacecraft

Figure 8. Contour Plots of Voltage in $\log_{10}(V)$ vs. Formation Size ($A_0$) and Debye Length for All Differential Perturbations. The Formation Consists of 2, 4 and 5 Craft at GEO.

15

Aluminum (or any light metal). The deputy satellite is assumed to be spherical with a fixed radius $r_1$ and mass $m_1$. Note, the size of the shell in the gluon is varied as part of the study. Hence, the mass of the gluon is not fixed and depends on the radius of the craft

$$m_2 = m_c + \left(8[2\pi r_h(r_2 - r_c)\Delta_h] + 4\pi r_2^2 \Delta_s\right)\rho_{al} \tag{26}$$

Here $r_2$, $r_c$ and $r_h$ are the radii of the shell, core mass and thin cylindrical columns, respectively. $\Delta_s$ and $\Delta_h$ denote the thickness of the shell and cylindrical column, and $\rho_{al}$ is the density of Aluminum.

*Voltage Requirements*

In this section, we find an expression for the amount of Coulomb force which will keep the formation from drifting due to the differential perturbation. The voltages on the gluon and deputy can be calculated from the magnitude of the Coulomb force required. Consider the Figure 9, let $\boldsymbol{F}_1$ and $\boldsymbol{F}_2$ be the external disturbance force acting on the deputy and gluon, respectively, and $\boldsymbol{F}_Q$ be the Coulomb force. The equation of motion of the two satellites are given as

$$\boldsymbol{F}_Q + \boldsymbol{F}_1 = m_1 \ddot{\boldsymbol{r}}_1 = m_1(\ddot{\boldsymbol{r}}_c + \ddot{\boldsymbol{\rho}}_1) \tag{27a}$$

$$-\boldsymbol{F}_Q + \boldsymbol{F}_2 = m_2 \ddot{\boldsymbol{r}}_2 = m_2(\ddot{\boldsymbol{r}}_c + \ddot{\boldsymbol{\rho}}_2) \tag{27b}$$

where $\boldsymbol{r}_c$ is the inertial position vector of the center of mass, and, $\boldsymbol{\rho}_1$ and $\boldsymbol{\rho}_2$ are the position vectors of the deputy and gluon with respect to the center of mass, respectively.
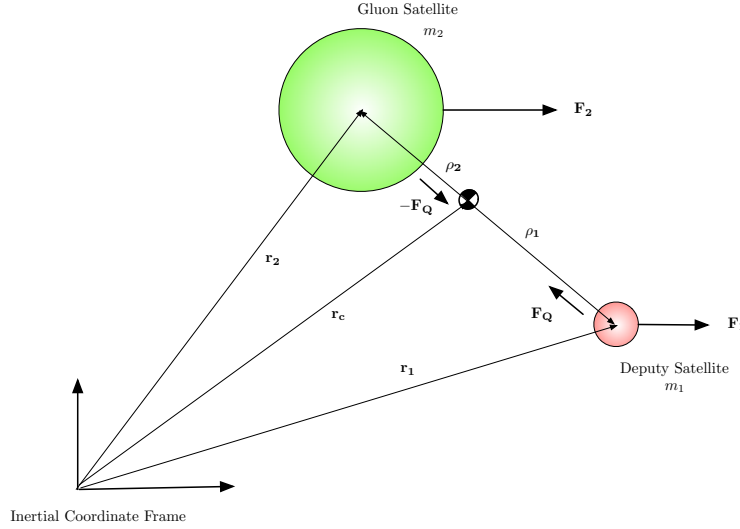


Figure 9. A simple gluon and deputy satellite illustration.

The net effect of the Coulomb forces on the center of mass is zero and its equation of motion is given by

$$(m_1 + m_2)\ddot{\boldsymbol{r}}_c = \boldsymbol{F}_1 + \boldsymbol{F}_2 \tag{28}$$

In order to keep the formation from drifting, we should generate a Coulomb force $\boldsymbol{F}_Q$, which will make $\ddot{\boldsymbol{\rho}}_1$ and $\ddot{\boldsymbol{\rho}}_2$ go to zero. By setting $\ddot{\boldsymbol{\rho}}_1$ as zero in Eq. (27a) and solving for $\boldsymbol{F}_Q$, we get

$$\boldsymbol{F}_Q = -\boldsymbol{F}_1 + m_1 \ddot{\boldsymbol{r}}_1 \tag{29}$$

16

In Eq. (29), Substituting for $\boldsymbol{F}_1$ from the center of mass equation in Eq. (28), we get

$$\boldsymbol{F}_Q = -\frac{m_2}{m_1 + m_2}\boldsymbol{F}_1 + \frac{m_1}{m_1 + m_2}\boldsymbol{F}_2 \tag{30}$$

The external forces, $\boldsymbol{F}_1$ and $\boldsymbol{F}_2$, in Eq. (30) can be rewritten in terms of acceleration as

$$\boldsymbol{F}_Q = \frac{m_1 m_2}{m_1 + m_2}(\boldsymbol{a}_2 - \boldsymbol{a}_1) \tag{31}$$

where, $\boldsymbol{a}_2$ and $\boldsymbol{a}_2$ are the inertial accelerations due to the external disturbance force. By writing out the full expression for the Coulomb force in Eq. (31) and equating the magnitudes of the force, we get

$$k_c \frac{q_1 q_2 e^{\left(\frac{-d}{\lambda_d}\right)}}{d^2} = \frac{m_1 m_2}{m_1 + m_2}a_d \tag{32}$$

where $a_d$ is the differential acceleration, $\lambda_d$ is the Debye length, $d$ is the separation distance between the satellites and, $q_1$ and $q_2$ are the charges of deputy and gluon respectively. By using the voltage-charge relationship in Eq. 18, we rewrite Eq. 32 as

$$\frac{r_1 r_2 V_1 V_2 e^{\left(\frac{-d}{\lambda_d}\right)}}{k_c d^2} = \frac{m_1 m_2}{m_1 + m_2}a_d \tag{33}$$

In general, the voltage on the gluon will be fixed and the voltage on the deputy will be varied to compensate for the differential drag. But, in this paper we have fixed the voltage of the deputy as 10 kV (maximum permissible) and varied the gluon voltage to see if it is below the available voltage. This is because the gluon size has not been fixed and we are interested in studying the gluon voltage-size and differential perturbation-size relationships. Solving Eq. 33 for $V_2$, we get

$$V_2 = \left(\frac{m_1 m_2}{m_1 + m_2}\right)\frac{k_c d^2 a_d}{r_1 r_2 V_1 e^{\left(\frac{-d}{\lambda_d}\right)}} \tag{34}$$

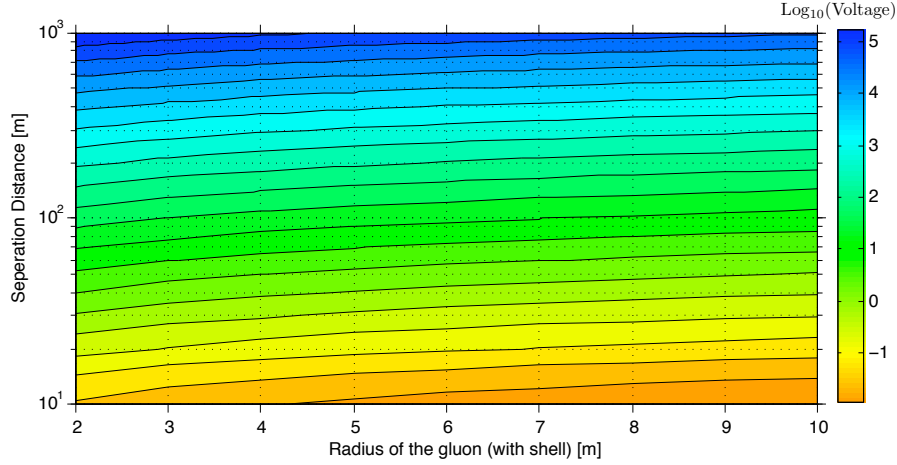*Differential Perturbations and Associated Voltages for Variable Gluon Radius*

Both the deputy satellite and gluon experience perturbations due to solar drag, atmospheric drag and $J_2$ effect. But, these perturbations are not equal in magnitude and cause a net force which may result in the drifting of the satellite formation. This differential perturbation depends on the mass, surface area and separation distance between the gluon and deputy. In an effort to study this dependence, we vary the gluon radius and separation distance and study the resulting differential perturbation. Due to similar Debye length limitations, the satellites are assumed to at GEO (fixed altitude of 35000 m).

Contours of voltage $V_2$ needed on the gluon to compensate for the differential solar drag, assuming a fixed deputy voltage $V_1$ (10 kV) is shown in Figure 10(a). Even though the differential solar radiation drag is less for smaller gluon radii, the voltage needed will increase because the smaller radii causes a higher charge density. After reaching a low around the 5 meter radius, there is a gentle increase in required voltage needed due to the increasing differential solar radiation perturbation. Contours of required gluon voltage $V_2$ needed to compensate for the differential $J_2$ effect, assuming a fixed deputy voltage $V_1$ (10 kV), is shown in Figure 10(b). The voltage needed increases with separation distance and gently decreases with increasing gluon radii.

In Figure 11 the required Gluon voltage levels are computed to allow the 10 kV charged deputy to compensate for all differential orbital perturbations acting on it at GEO. The Debye lengths are varied to illustrate the gluon voltages at different HEO plasma level conditions. For craft flying up to 30 meters apart, the voltages rise up to kV levels. As the Debye lengths are reduced, the voltage increase even further.

17
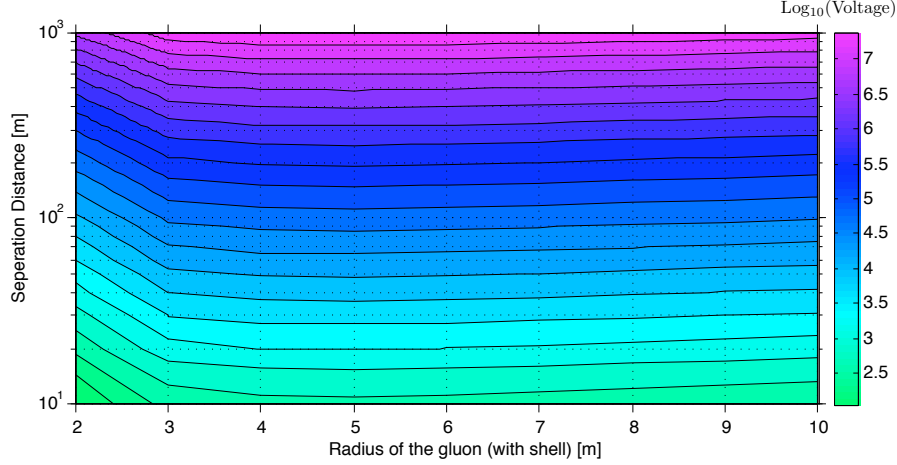
(a) Gluon voltage $V_2$ needed for the differential solar drag.



(b) Gluon voltage $V_2$ needed on the gluon to compensate for the differential $J_2$ effect.

Figure 10. Differential Perturbations at GEO (fixed altitude of 35000 km and a Debye length of 500 meters). All values are $log_{10}$ of voltages.

## CONCLUSION

In this paper we examine the effects of several types of perturbations on the relative motion of closely-flying satellites. The worst case differential accelerations are estimated relative to the drifting formation center of mass for $J_2$, atmospheric and solar radiation drag cases. In particular, very small separation distances ranging from 10–1000 meters are considered from LEO to GEO altitudes. The results illustrate that differential solar radiation drag will be the most significant differential perturbation at higher Earth orbits for Coulomb spacecraft.

Studying the Lorentz force, we observed that accelerations due to the Earth's magnetic field and a spacecraft charge will be less than most of the perturbations for high Earth orbits, but can become a significant force if the spacecraft charges grow too large. Further, a study is performed to investigate minimum required spacecraft charged to compensate for these differential perturbations. Two cases are considered. First, all craft are aligned in a traditional bounded Hill frame formation and allowed to interact with each other. Second, the case is considered where a large gluon spacecraft is created
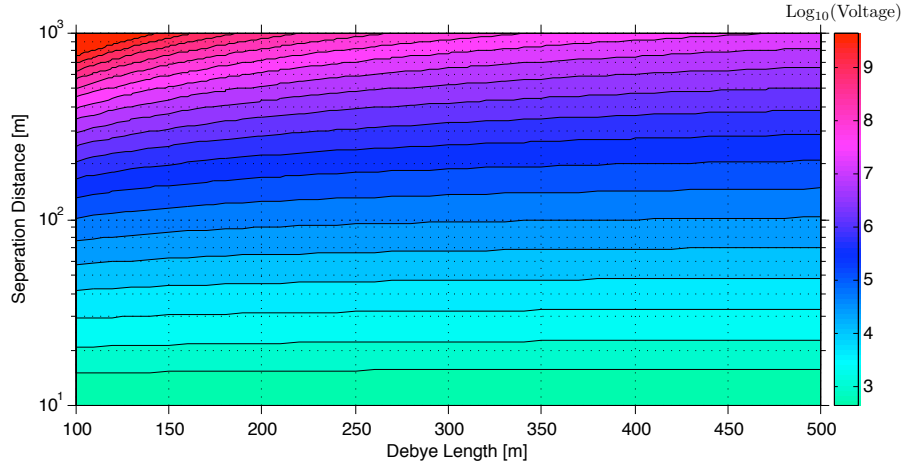
18

Figure 11. Voltage $V_2$ needed on gluon to compensate for all the differential perturbations with a Gluon radius of 10 meters. All values are $log_{10}$ of voltages.

which is capable of achieving high voltages. Here the deputy spacecraft will only interact with the gluon spacecraft. Numerical studies illustrated expected orbit maintenance voltage levels. For orbits with dozens of meters separation distances the craft must charge up to kilovolt levels.

## ACKNOWLEDGMENT

## REFERENCES

[1] C. C. Chao, "Long-term Orbit Perturbations of the DRAIM 4 Satellite Constellations.," *Journal of Guidance Control and Dynamics*, Vol. 15, No. 6, 1992, pp. 1406–1410.

[2] L. B. King, G. G. Parker, S. Deshmukh, and J.-H. Chong, "Spacecraft Formation-Flying using Inter-Vehicle Coulomb Forces," tech. rep., NASA/NIAC, January 2002. `http://www.niac.usra.edu`.

[3] L. B. King, G. G. Parker, S. Deshmukh, and J.-H. Chong, "Study of Interspacecraft Coulomb Forces and Implications for Formation Flying," *AIAA Journal of Propulsion and Power*, Vol. 19, May–June 2003, pp. 497–505.

[4] A. Juhasz and M. Horanyi, "Dynamics of charged space debris in the Earth's plasma environment," *Journal of Geophysical Research*, Vol. 102, April 1997, pp. 7237–7246.

[5] H. B. Garrett and S. E. DeForest, "An Analytical Simulation of the Geosynchronous Plasma Environment," *Planetary Space Science*, Vol. 27, 1979, pp. 1101–1109.

[6] T. E. Craven, *Physics of Solar System Plasmas*. Cambridge University Press, 1997.

[7] G. W. Hill, "Researches in the Lunar Theory," *American Journal of Mathematics*, Vol. 1, No. 1, 1878, pp. 5–26.

[8] W. H. Clohessy and R. S. Wiltshire, "Terminal Guidance System for Satellite Rendezvous," *Journal of the Aerospace Sciences*, Vol. 27, Sept. 1960, pp. 653–658.

[9] H. Schaub and J. L. Junkins, *Analytical Mechanics of Space Systems*. Reston, VA: AIAA Education Series, October 2003.

[10] R. Sedwick, D. Miller, and E. Kong, "Mitigation of Differential Perturbations in Clusters of Formation Flying Satellites," *AAS/AIAA Space Flight Mechanics Meeting*, February 1999. Paper No. AAS 99-124.

[11] V. Kapila, A. G. Sparks, J. M. Buffington, and Q. Yan, "Spacecraft Formation Flying: Dynamics and Control," *Proceedings of the American Control Conference*, San Diego, California, June 1999, pp. 4137–4141.

[12] K. T. Alfriend and H. Schaub, "Dynamics and Control of Spacecraft Formations: Challenges and Some Solutions," *Journal of the Astronautical Sciences*, Vol. 48, April–Sept. 2000, pp. 249–267.

[13] R. Burns, C. A. McLaughlin, J. Leitner, and M. Martin, "TechSat 21: formation design, control, and simulation," *IEEE Aerospace Conference Proceedings*, Vol. 7, Big Sky, MO, March 18–25 2000, pp. 19–25.

[14] R. H. Battin, *An Introduction to the Mathematics and Methods of Astrodynamics*. New York: AIAA Education Series, 1987.

[15] A. E. Roy, *Orbital Motion*. Adam Hilger Ltd, Bristol, England, 2nd ed., 1982.

[16] U. G. P. Office, "U.S. Standard Atmosphere," Washington, D.C., 1976.

[17] J. R. Wertz and W. J. Larson, *Space Mission Analysis and Design*. Dordrecht, The Netherlands: Kluwer Academic Publishers, 1991.

[18] K. Toshihiro, "Solar radiation pressure model for the relay satellite of selene," *Earth Space and Planets*, Vol. 51, September 1999, pp. 979–986.

[19] H. Schaub and K. T. Alfriend, "$J_2$ Invariant Relative Orbits for Spacecraft Formations," *Celestial Mechanics and Dynamical Astronomy*, Vol. 79, No. 2, 2001, pp. 77–95.

[20] P. Sengupta and S. R. Vadali, "A Lyapunov-Based Controller for Satellite Formation Reconfiguration in the Presence of $J_2$ Perturbations," *AAS Space Flight Mechanics Meeting*, Maui, Hawaii, February 8–12 2004. Paper No. AAS-04-253.

[21] K. T. Alfriend, H. Schaub, and D.-W. Gim, "Gravitational Perturbations, Nonlinearity and Circular Orbit Assumption Effect on Formation Flying Control Strategies," *Proceedings of the Annual AAS Rocky Mountain Conference*, Breckenridge, CO, Feb. 2–6 2000, pp. 139–158.

[22] K. L. Makovec, "A Nonlinear Magnetic Controller for Three-Axis Stability of Nanosatellites," Master's thesis, Virginia Polytechnic Institute and State University, Blacksburg, VA, July 2001.

[23] H. Schaub, G. G. Parker, and L. B. King, "Challenges and Prospect of Coulomb Formations," *Journal of the Astronautical Sciences*, Vol. 52, Jan.–June 2004, pp. 169–193.

[24] E. M. Kong, D. W. Miller, and R. J. Sedwick, "Optimal Trajectories and Orbit Design for Separated Spacecraft Interferometry," tech. rep., Massachusetts Institute of Technology, November 1998. SERC #13–98.

[25] S. R. Vadali, K. T. Alfriend, and S. Vaddi, "Hill's Equations, Mean Orbit Elements, and Formation Flying of Satellites," *The Richard H. Battin Astrodynamics Conference*, College Station, TX, March 2000. Paper No. AAS 00-258.

[26] E. Kong, D. W. Miller, and R. J. Sedwick, "Exploiting Orbital Dynamics for Aperture Synthesis using Distributed Satellite Systems," *Proceedings of the Space Flight Mechanics Meeting*, Breckenridge, CO, Feb. 7–10 1999, pp. 385–301. Paper AAS-99-112.

[27] H. Schaub, S. R. Vadali, and K. T. Alfriend, "Spacecraft Formation Flying Control Using Mean Orbit Elements," *Journal of the Astronautical Sciences*, Vol. 48, No. 1, 2000, pp. 69–87.